AJNR

Quantitative Diffusion-Weighted and Dynamic Susceptibility-Weighted Contrast-Enhanced Perfusion MR Imaging Analysis of T2 Hypointense Lesion Components in Pediatric Diffuse Intrinsic Pontine Glioma

U. Löbel, J. Sedlacik, W.E. Reddick, M. Kocak, Q. Ji, A. Broniscer, C.M. Hillenbrand and Z. Patay

AJNR Am J Neuroradiol published online 18 November 2010
http://www.ajnr.org/content/early/2010/11/18/ajnr.A2277.citation

Published November 18, 2010 as 10.3174/ajnr.A2277

Quantitative Diffusion-Weighted and Dynamic Susceptibility-Weighted Contrast-Enhanced Perfusion MR Imaging Analysis of T2 Hypointense Lesion Components in Pediatric Diffuse Intrinsic Pontine Glioma

ORIGINAL RESEARCH

U. Löbel
J. Sedlacik
W.E. Reddick
M. Kocak
Q. Ji
A. Broniscer
C.M. Hillenbrand
Z. Patay

BACKGROUND AND PURPOSE: Focal anaplasia characterized by T2 hypointensity, signal-intensity enhancement on postcontrast T1-weighted MR imaging and restricted water diffusion has been reported in a patient with juvenile pilocytic astrocytoma. We identified $T2_{HOF}$ with these MR imaging characteristics in children with DIPG and hypothesized that these represent areas of focal anaplasia; and may, therefore, have increased perfusion properties and should be characterized by increased perfusion. Thus, we used DSC to investigate our hypothesis.

MATERIALS AND METHODS: We retrospectively reviewed the baseline MR imaging scans of 86 patients (49 girls, 37 boys; median age, 6.1 years; range, 1.1–17.6 years) treated for DIPG at our hospital (2004–2009). $T2_{HOF}$ with the described MR imaging characteristics was identified in 10 patients. We used a region of interest–based approach to compare the ADC, FA, rCBV, rCBF, and rMTT of $T2_{HOF}$ with those of the typical $T2^{HRT}$.

RESULTS: The ADC of $T2_{HOF}$ with the specified MR imaging characteristics was significantly lower than that of $T2^{HRT}$ (range, 0.71–1.95 μm^2/ms versus 1.36–2.13 μm^2/ms; $P < .01$); and the FA (range, 0.12–0.34 versus 0.07–0.24; $P = .03$) and rCBV (range, 0.4–2.62 versus 0.23–1.57; $P = .01$) values of $T2_{HOF}$s were significantly higher.

CONCLUSIONS: Our data suggest that $T2_{HOF}$ in DIPG may represent areas of focal anaplasia and underline the importance of regional, rather than global, tumor-field analysis. $T2_{HOF}$ may be the ideal target when stereotactic biopsy of tumors that present with an inhomogeneous T2 signal intensity is considered.

ABBREVIATIONS: ADC = apparent diffusion coefficient; AIF = arterial input function; a.u. = arbitrary units; CBF = cerebral blood flow; CBV = cerebral blood volume; DIPG = diffuse intrinsic pontine glioma; DSC = dynamic susceptibility-weighted contrast-enhanced perfusion MR imaging; DTI = diffusion tensor imaging; DWI = diffusion-weighted imaging; FA = fractional anisotropy; GBCA = gadolinium-based contrast agent; GM = gray matter; rCBF = relative cerebral blood flow; rCBV = relative cerebral blood volume; rMTT = relative mean transit time; $T2_{HOF}$ = T2 hypointense focus with postcontrast signal enhancement and diffusion restriction; $T2^{HRT}$ = typical T2 hyperintense tumor; WM = white matter

PEDIATRICS

ORIGINAL RESEARCH

In children, tumors arising from the brain stem (ie, midbrain, pons, and medulla oblongata) account for approximately 11% of all central nervous system tumors.[1] Approximately 58%–85% of the tumors in this category correspond to DIPG, an entity associated with a distinctively poor prognosis.[2-4] Available literature suggests that at least a subset of these tumors is histologically low grade (ie, World Health Organization grade II) at initial clinical presentation[5,6] but rapidly evolves into high-grade neoplasms, with most found to be glioblastoma multiforme at postmortem examination.[7,8]

A recent case of a histologically confirmed focal anaplasia within a cerebellar juvenile pilocytic astrocytoma showed a peculiar constellation of MR imaging signal-intensity properties, notably shortened T2 relaxation (ie, hyposignal), signal-intensity enhancement after injection of a GBCA, and evidence of restricted water diffusion (ie, increased signal intensity on diffusion trace images in conjunction with low ADC).[9] During the course of providing clinical care for patients with DIPG, we have occasionally seen focal intratumoral lesions characterized by the aforementioned MR imaging features. We, therefore, speculated that these lesions may represent focal anaplasia and have prognostic and therapeutic implications.

Current standards for the clinical management of DIPG, including those at our hospital, do not require histopathologic confirmation before treatment. Furthermore, the use of invasive biopsies to confirm suspected cases of DIPG remains

Received May 25, 2010; accepted after revision July 13.

From the Departments of Radiological Sciences (U.L., J.S., Q.J., C.M.H., W.E.R., Z.P.), Biostatistics (M.K.), and Oncology (A.B.), St. Jude Children's Research Hospital, Memphis, Tennessee.

This work was supported by the American Lebanese Syrian Associated Charities. A. Broniscer was supported by Astra Zeneca.

Paper previously presented at: Annual Meeting of the American Society of Neuroradiology, May 15–20, 2010; Boston, Massachusetts; and presented in part at: Annual Meeting of the European Society of Neuroradiology, September 17–20, 2009; Athens, Greece.

Please address correspondence to Zoltan Patay, MD, PhD, Division of Neuroradiology, Department of Radiological Sciences, St. Jude Children's Research Hospital, 262 Danny Thomas Pl, Mail Stop 220, Memphis, TN 38105-2794; e-mail: zoltan.patay@stjude.org

DOI 10.3174/ajnr.A2277

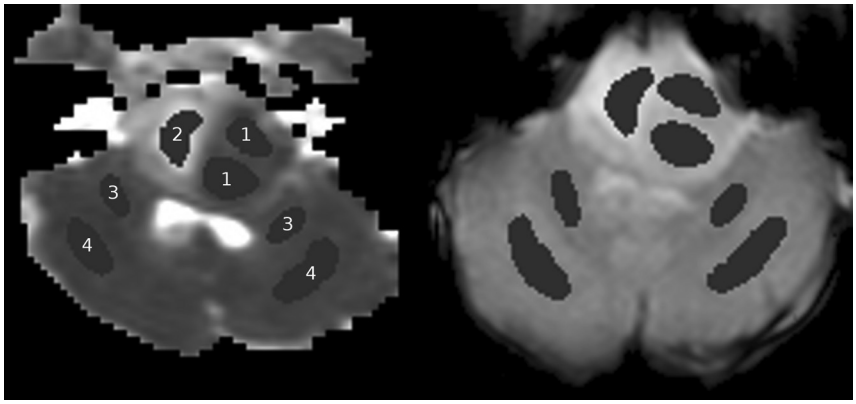

Fig 1. Regions of interest for $T2_{HOF}$ (1), $T2^{HRT}$ (2), WM (3), and GM (4) shown on the ADC map (left) and the T2*-weighted perfusion image before injection of contrast agent (right).

controversial,[10] mainly due to the highly characteristic MR imaging features of this disease in most cases and the almost uniformly poor prognosis. Therefore, testing our hypothesis through histopathologic evaluation appeared to be impossible. However, because the histologic hallmark features of anaplasia are angioneogenesis and hypercellularity and advanced MR imaging techniques can provide robust in vivo surrogate parametric data about tumor cellularity (eg, ADC) and vascularity (eg, CBV), which correlate with tumor grade and clinical outcome,[11-16] we used DWI, DTI (in some cases), and DSC to further characterize $T2_{HOF}$. Our goal was to determine the diffusion and perfusion properties of $T2_{HOF}$ within DIPGs and to compare these with those of the $T2^{HRT}$.

Materials and Methods

Patients

Pretreatment MR images of 86 patients with DIPG (49 girls, 37 boys; median age at diagnosis, 6.1 years; range, 1.1–17.6 years) who were admitted to our hospital between 2004 and 2009 were retrospectively reviewed for the presence of $T2_{HOF}$ associated with signal-intensity enhancement on T1-weighted postcontrast images and for evidence of restricted water diffusion by DWI. $T2_{HOF}$ with the described MR imaging characteristics was identified in 10 patients. T2*-weighted gradient-echo imaging or susceptibility-weighted imaging was used to ensure that hemorrhagic lesions were excluded. Informed consent from the parents or legal representatives of patients was obtained before performing MR imaging. The retrospective evaluation of the MR imaging data was approved by the local institutional review board. Qualifying $T2_{HOF}$ was categorized into 3 subgroups on the basis of appearance on the T2-weighted image: 1) a homogeneous lesion with well-defined margins, 2) a homogeneous lesion with ill-defined margins, and 3) an ill-defined lesion with evidence of central necrosis.

MR Imaging

Because the study spanned 5 years, MR imaging examinations were performed on 1.5T (3 patients; MAGNETOM Avanto, MAGNETOM Symphony; Siemens, Erlangen, Germany) and 3T (7 patients; MAGNETOM Trio, Siemens) MR imaging scanners. All patients, except patient 9, were under general anesthesia during the studies.

MR imaging protocols included nonenhanced axial T1-weighted gradient-echo, axial T2-weighted fast spin-echo, and axial echo-planar DWI (or DTI for patients 3 and 6–10) as well as axial contrast-enhanced T1-weighted gradient-echo imaging. Conventional anatomic images were used for the initial retrospective review to identify potential $T2_{HOF}$ within our cohort.

To enhance the visibility of any subtle signal-intensity enhancement within the $T2_{HOF}$ after intravenous injection of a GBCA, we subtracted nonenhanced T1-weighted images from postcontrast T1-weighted images by using the standard proprietary in-line subtraction algorithm available on our MR imaging platforms.

Diffusion MR Imaging

Patients in this study were initially enrolled into various clinical therapeutic trials. Depending on the corresponding treatment protocol, we acquired DWI data by using either DWI or DTI. Both diffusion-weighted sequences were performed by using a twice-refocused spin-echo technique. DWI was performed with 3 orthogonal diffusion-encoding directions, and DTI, with 12 directions. The b-values were 1000 and 700 s/mm^2 for the 1.5T and 3T scanners, respectively. ADC and FA maps were calculated by using the diffusion toolbox for SPM2 (Wellcome Department of Imaging Neuroscience, London, United Kingdom).

Perfusion MR Imaging

DSC data were acquired by using an echo-planar imaging sequence after an intravenous injection of a bolus of GBCA (at a dose of 0.1 mL/kg; Omniscan, Nycomed Amersham, Oslo, Norway; or Magnevist, Schering, Berlin, Germany), which was delivered by a power injector through a 22-ga intravenous line at a rate of 0.8–1.0 mL/s. The tumor was preloaded approximately 3 minutes prior to the scan with the same dose and injection rate. The DSC image acquisition started approximately 35–40 seconds before the contrast agent entered the intracranial space and ended after a few recirculation passes of contrast, with the first pass roughly in the middle of the acquisition. Parameters used for perfusion measurements were the following: TE = 28 ms for 3T, TE = 45 ms for 1.5T, TR = 1800 ms, matrix, 128 × 128, FOV = 210 × 210 mm^2, 15 sections with 5-mm thickness and 1-mm distance.

Collection of Quantitative Data

A region of interest–based approach was used to compare diffusion and perfusion parameters of $T2_{HOF}$ with $T2^{HRT}$. All regions of interest were drawn by 1 author (U.L.) under the supervision of a certified neuroradiologist (Z.P.). $T2_{HOF}$ was outlined on ADC maps, and regions of interest were transferred to non-contrast-enhanced T2*-weighted perfusion stack images (Fig 1). Reference regions of interest representing $T2^{HRT}$ were placed in a contralateral mirror tumor location whenever possible. When this was not possible because of obvious necrosis, hemorrhage, or central location of the $T2_{HOF}$, the

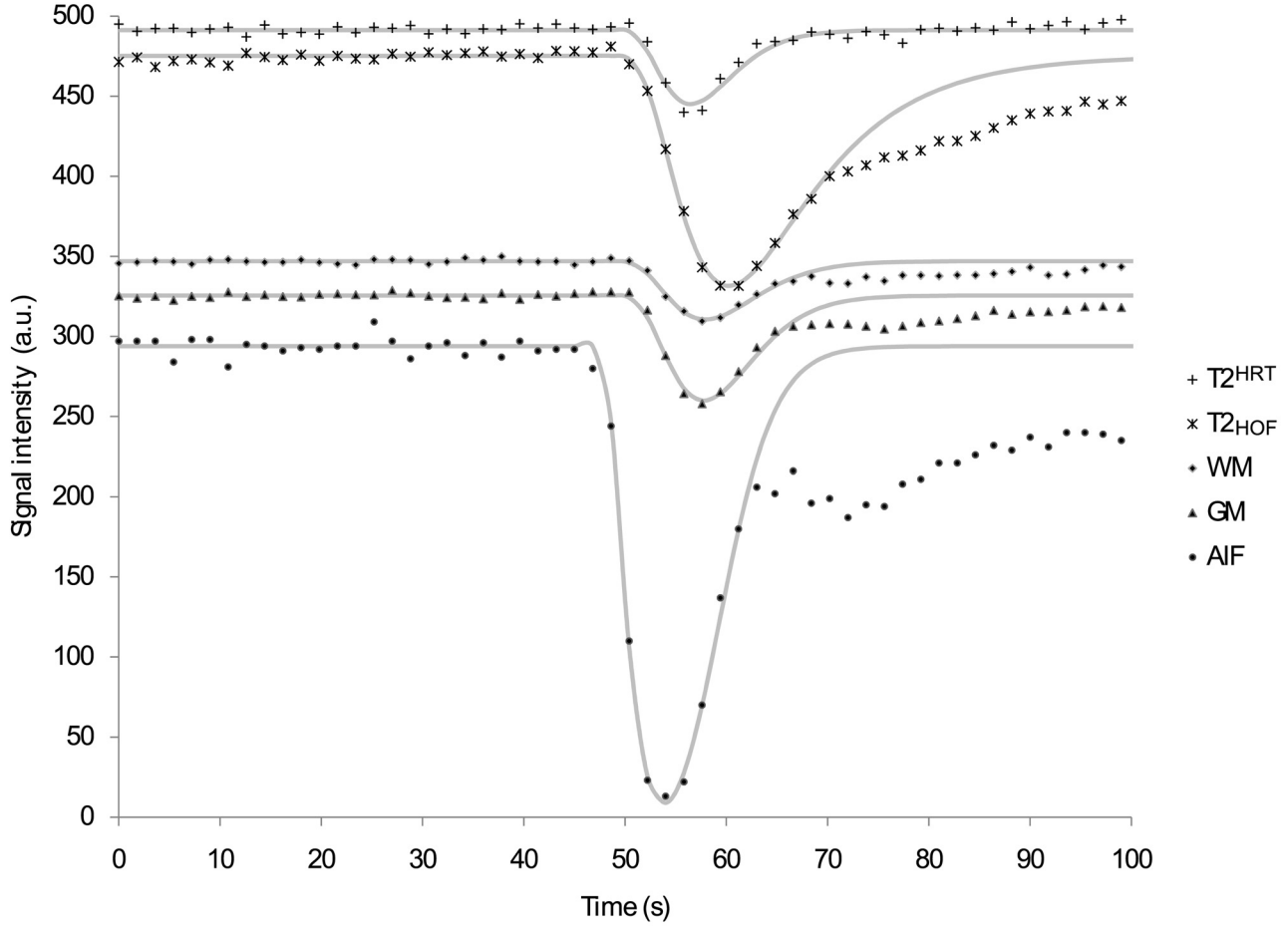

Fig 2. Signal-intensity curves of the tumor areas ($T2_{HOF}$ and $T2^{HRT}$), the normal-appearing cerebellar WM and GM, and the AIF for a single patient. The markers indicate the actual values measured; the lines indicate the fit functions to the first pass of the contrast agent.

region of interest was drawn in another representative (ie, fairly homogeneously T2 hyperintense) tumor area. Regions of interest for $T2^{HRT}$ were defined at a size similar to that of the regions of interest for $T2_{HOF}$, and a sufficient distance was kept to the rim of the brain stem to ensure that possible signal-intensity distortions were not included in the regions of interest. Regions of interest of normal-appearing cerebellar GM and WM were placed bilaterally (Fig 1).

Diffusion data were evaluated on the basis of the median pixel value of the ADC and FA maps for each region of interest calculated by using a self-written script in Matlab (MathWorks, Natick, Massachusetts).

The raw DSC–MR imaging dataset was initially processed by using a Kohonen self-organizing map to robustly and automatically identify the normalized AIF.[17] We decided against using a region-of-interest analysis of the final processed parameter maps because the pixel-wise evaluation often did not converge, and many of the voxels in the brain stem yielded illogical results. To determine specific perfusion parameters (ie, CBV, CBF, and MTT), we evaluated the signal intensity−time curve of each region of interest (Fig 2)[18] by using a more robust model-dependent deconvolution technique. This evaluation was performed by fitting the perfusion model with the monoexponential residue function to the first pass of the contrast bolus of the DSC data of each region of interest.[19] Relative CBV and relative CBF values were calculated by using the mean values obtained for both GM[20] regions of interest of the normal-appearing cerebellum. GM was chosen because DSC measures in this region are more reliable and less variable than those in WM regions of the cerebellum.

Statistical Evaluation

Statistical analyses involved comparing descriptive statistics and using graphic tools as well as the Wilcoxon signed rank test to evaluate the differences between the diffusion and perfusion parameters of $T2_{HOF}$ and $T2^{HRT}$. For patients with multiple $T2_{HOF}$, 1 lesion (ie, the index lesion) was used for descriptive statistics and comparative statistical analysis of the imaging features of a $T2_{HOF}$ versus a $T2^{HRT}$ field (Table, last column). We selected the index lesion on the basis of the robustness of the defining $T2_{HOF}$ imaging features in that lesion.

Results

Reviewing the images of our patients, we identified 15 instances of $T2_{HOF}$ in 10 patients that fully met the MR imaging criteria described previously. Of the 10 patients (6 boys, 4 girls; median age at diagnosis, 4.6 years; range, 1.2–13.1 years), 7 patients had a single $T2_{HOF}$, and 3 patients had 2 lesions (Table, Fig 3). DSC data were available for all 10 patients. The initial MR imaging study of patient 8 did not include diffusion imaging, so the scan obtained 5 days after initiation of treatment was evaluated. FA values were available for patients 3 and 6–10. Signal-intensity enhancement on post-contrast T1-weighted images was usually subtle to modest but

Summary of data obtained for 10 patients

No.	Age (yr)	Sex	Lesion Category	ADC (μm^2/ms) (Median)				FA (Median)				rCBV		rCBF		MTT		Index Lesion[a]
				$T2_{HOF}$	$T2^{HRT}$	WM	GM	$T2_{HOF}$	$T2^{HRT}$	WM	GM	$T2_{HOF}$	$T2^{HRT}$	$T2_{HOF}$	$T2^{HRT}$	$T2_{HOF}$	$T2^{HRT}$	
1	4.6	M	2	1.49	1.96	0.90	0.93					1.45	1.12	0.93	0.93	1.75	1.32	x
2	3.6	F	3	1.04	1.70	0.71	0.73					0.96	1.00	0.34	0.55	3.50	1.99	x
			3	0.89	1.70	0.71	0.73					0.77	1.00	0.56	0.55	1.44	1.99	
3	1.2	M	2	1.36	2.13	0.80	0.87	0.27	0.16	0.58	0.23	0.59	0.57	1.11	0.63	0.49	0.88	
			1	1.38	2.13	0.80	0.87	0.34	0.16	0.58	0.23	0.98	0.57	0.90	0.63	1.03	0.88	x
4	5.7	M	3	0.88	1.71	0.78	0.70					2.62	1.17	1.19	0.84	2.27	1.41	x
5	3.7	F	3	0.81	1.46	0.73	0.75					1.66	0.75	0.71	0.59	2.37	1.28	x
6	3.6	F	1	1.95	2.02	0.78	0.79	0.12	0.07	0.38	0.25	0.94	0.45	0.41	0.47	2.52	0.94	x
7	4.6	M	1	1.18	1.65	0.82	0.76	0.31	0.12	0.42	0.24	0.40	0.23	0.30	0.27	1.37	0.84	x
8	8.9	F	2	0.71	1.92	0.73	0.69	0.22	0.08	0.28	0.22	2.39	0.38	1.19	0.73	2.89	0.50	x
			2	0.76	1.92	0.73	0.69	0.33	0.08	0.28	0.22	2.19	0.38	1.88	0.73	1.17	0.50	
9	13.1	M	2	1.04	1.36	0.74	0.75	0.21	0.24	0.42	0.29	2.07	1.57	1.49	0.55	1.45	4.43	x
10	9.4	M	2	1.02	1.53	0.71	0.88	0.21	0.12	0.51	0.25	1.05	1.25	1.32	1.64	0.78	0.74	x

[a] Lesions marked with x are used for calculation of *P* values.

was more prominent in those lesions associated with central necrosis.

The regions of interest used for data evaluation had an average size of 270 pixels. The smallest region of interest was drawn for a $T2_{HOF}$ and was 52 pixels. The largest region of interest was drawn for the cerebellar GM and was 1024 pixels for both bilateral regions of interest combined.

Diffusion MR Imaging

Median ADC values of the 10 index lesions ranged from 0.71 to 1.95 μm^2/ms and were significantly lower ($P < .01$) than the ADC values obtained in $T2^{HRT}$, which ranged from 1.36 to 2.13 μm^2/ms. Median ADC values of cerebellar WM ranged from 0.71 to 0.90 μm^2/ms, and median ADC values of cerebellar GM ranged from 0.69 to 0.93 μm^2/ms.

Median FA values of the 6 index lesions for which FA could be calculated ranged from 0.12 to 0.34 and were significantly higher ($P = .03$) than the values obtained for the $T2^{HRT}$ field (range, 0.07–0.24) in our patient cohort. Median FA values of cerebellar WM ranged from 0.28 to 0.58, and median FA values of cerebellar GM ranged from 0.22 to 0.29. These results are summarized in Fig 4.

Perfusion MR Imaging

Representative DSC data of 1 patient and the fitted model curve for each region of interest are shown in Fig 2. The comparison of $T2_{HOF}$ and $T2^{HRT}$ by using DSC showed that the rCBV was significantly higher ($P = .01$) in $T2_{HOF}$ (range, 0.4–2.62) than in $T2^{HRT}$ (range, 0.23–1.57). In contrast, values for rCBF and rMTT were not significantly different between the 2 groups; these results are summarized in Fig 5.

Discussion

We found that the MR imaging appearance of $T2_{HOF}$ is not entirely uniform. While some of the lesions were fairly well-defined, others were ill-defined, often larger, with or without evidence of central necrosis.

We believe that the finding of lower ADC values in $T2_{HOF}$ compared with those of $T2^{HRT}$ likely indicates increased cellular attenuation and a high nucleus-to-cytoplasm ratio,[21] which is in accordance with the well-documented inverse correlation between ADC and tumor cellularity reported by other investigators.[22] ADC values for 8 of the 13 lesions (patients 2, 4, 5, and 8–10) in this study corresponded to values found in World Health Organization grade III and IV supratentorial gliomas in another study.[23] For patient 8, ADC values were as low as those reported for medulloblastoma, which is among the central nervous system tumors with the highest cellularity.[15]

Previous studies suggest that ADC alone does not enable differentiation between low-grade and high-grade gliomas.[12,23] Researchers investigating the diffusion parameter FA reported that a threshold value of 0.188 may differentiate low-grade from high-grade supratentorial gliomas.[23] On the basis of this threshold, 5 of the 6 examples of $T2_{HOF}$ for which FA was available would also correspond to high-grade lesions. Higher FA values observed in high-grade compared to low-grade gliomas has been associated with a symmetric organization of the cells within the hypercellular lesion.[23] ADC and FA values within the tumor and normal-appearing cerebellar WM (ie, the middle cerebellar peduncle) in our cohort are in agreement with the values in other reports.[24-26] Compared with normal values found for the pons in 5- to 10-year-old subjects,[27] ADC values were higher and FA values were lower in the $T2_{HOF}$ and $T2^{HRT}$ that we studied (the deviation from normal values was much more prominent in $T2^{HRT}$ than in $T2_{HOF}$).

DSC is the current MR imaging–based technique of choice for in vivo quantification of perfusion parameters within normal and abnormal biologic samples, including neoplasms.[11,14,16] Although no validated cutoff value for rMTT has been reported, increased rCBV is believed to closely reflect angioneogenesis, vascular endothelial proliferation, or vascular attenuation[11,28]; rCBV seems to be a reliable predictor of clinical outcome in adults with supratentorial brain neoplasms. In fact, rCBV is used as a surrogate biomarker to differentiate and grade intracranial masses.[28,29] Furthermore, rCBV values >1.75 identify neoplasms with poor patient outcome,[28] and, by using 2.91 as a cutoff value for rCBV, enable highly sensitive and specific differentiation of low-grade supratentorial gliomas from high-grade ones.[30] The rCBV values for $T2^{HRT}$ in our study agree with those reported for grade II and III supratentorial fibrillary astrocytomas.[18] In contrast, rCBV values of $T2_{HOF}$ were notably higher, which is in agreement with increased vascularity and, therefore, consistent with potential anaplasia.

The use of cutoff values for DSC data is currently limited because most available rCBV and rCBF cutoff values were

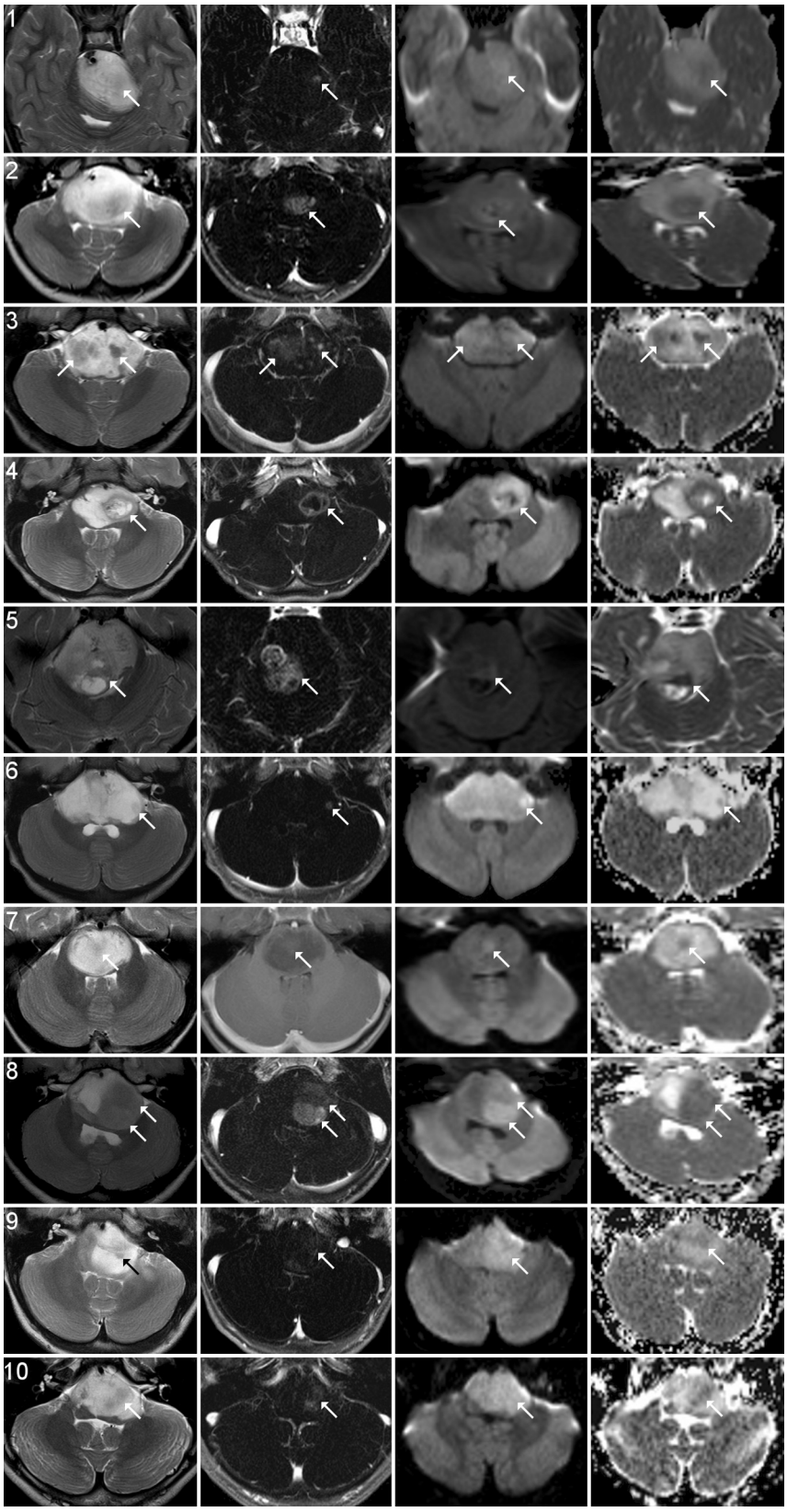

Fig 3. Appearance of $T2_{HOF}$ on conventional MR imaging and DWI for the 10 patients included in the evaluation of quantitative data. From left to right: T2-weighted, T1 subtraction image (or T1-weighted postcontrast image), diffusion trace image, and ADC map.

established for supratentorial gliomas relative to contralateral normal-appearing WM.[11,14,20,30,31] This approach was not feasible for our study because of the midline tumor location and because some DIPGs extended into the middle cerebellar peduncles.

One potential challenge to confidently identifying a $T2_{HOF}$ is differentiating it from other T2 hypointensities within the tumor field. Theoretically, those other T2 hypointensities may be hemorrhagic or normal, yet uninvolved, brain stem parenchyma. Identifying hemorrhagic foci is straightforward with

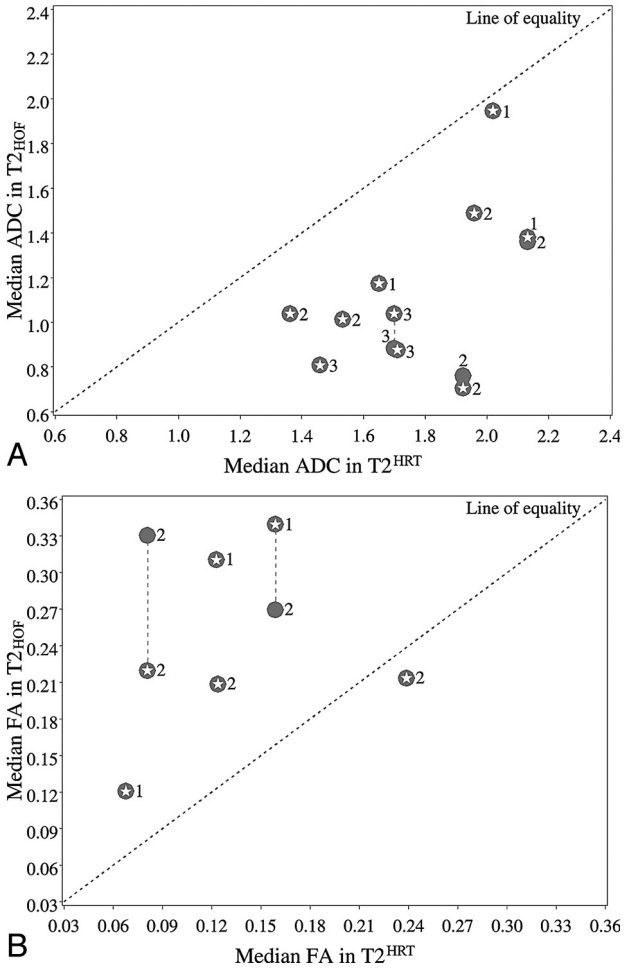

Fig 4. Results of diffusion imaging. *A*, ADC values of all lesions are significantly lower. *B*, FA values (not available for all patients) are significantly higher in $T2_{HOF}$ (y-axis) than in $T2^{HRT}$ (x-axis).

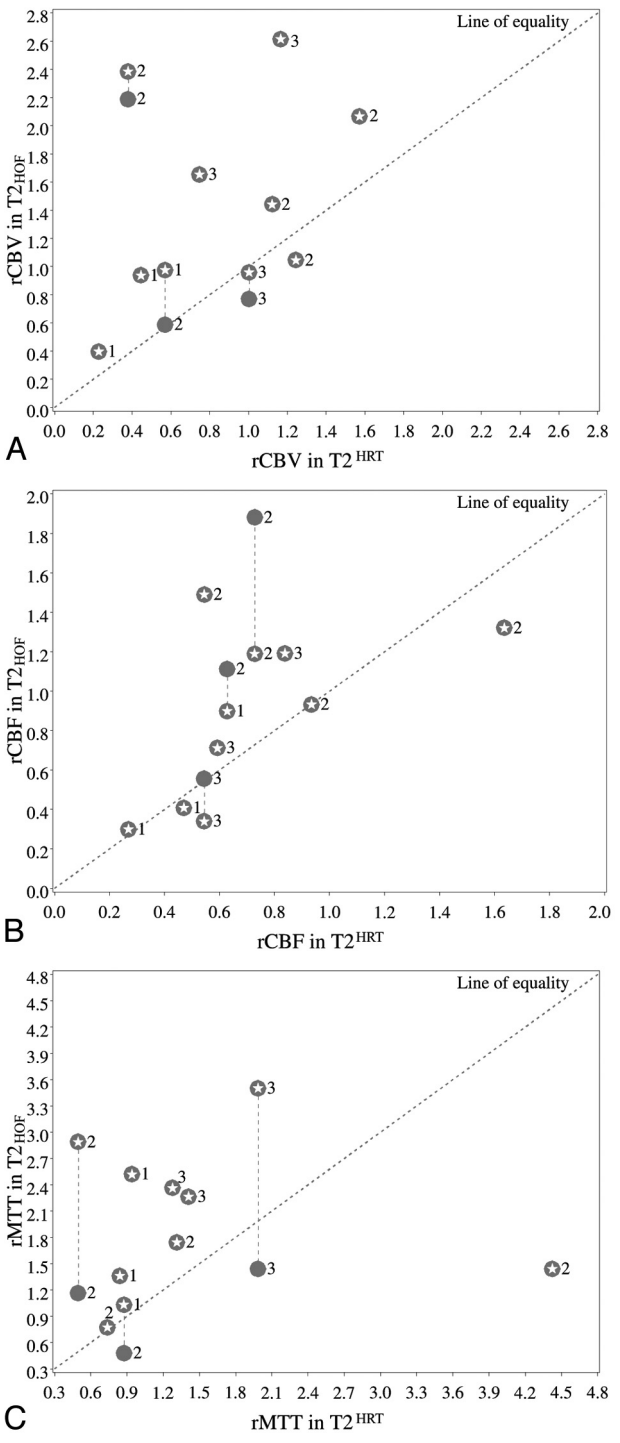

Fig 5. Results of perfusion imaging. *A*, rCBV values are significantly higher in $T2_{HOF}$ (y-axis) than in $T2^{HRT}$ (x-axis). *B* and *C*, No statistically significant difference is observed for (*B*) rCBF and (*C*) rMTT. Parameters were calculated relative to normal-appearing cerebellar GM.

the use of blood-sensitive sequences, particularly with susceptibility-weighted imaging.[32] Normal parenchyma is usually found in the periphery of the tumor; however because tumor geometry is often not strictly spheric, foci of normal parenchyma may appear partially intratumoral on axial images. Fiber tracts within the brain stem represent a special form of normal T2 hypointensities within the T2 hyperintense tumor field. Corticospinal tracts and transverse pontine fibers seem to be relatively resistant to tumor infiltration. Therefore, although these tracts and fibers are often splayed and quite significantly displaced by surrounding infiltrative tumor, they remain T2 hypointense. Their small size (1–2 mm), the resultant characteristic "ground pepper" appearance, and their suggestive locations within the ventral quadrants of the pons usually make their recognition straightforward. In cases in which confirmation is needed, DTI data showing marked anisotropy may further enhance diagnostic confidence.

Clinical Implications

Our findings highlight the potential usefulness of a regional rather than global analysis of the tumor field when using advanced MR imaging techniques, and they show the feasibility of using these techniques, even with relatively small lesion components in a challenging anatomic region such as the posterior fossa. Incidentally, our findings also suggest that unusual tumor features on conventional MR imaging, such as T2 hypointensities, may provide clues to the staging and biology of DIPG.

Histogenetic differences between pontine neoplasms, currently labeled uniformly as DIPG, may be responsible for rare but striking differences in the clinical course and therapeutic

responsiveness of some of these tumors.[11] More systematic access to tissue samples through surgical biopsy may be required to further differentiate DIPG from similar tumors and gain a better understanding of the molecular biology of DIPG. Yet, without appropriate imaging guidance, tumors may be randomly biopsied, thus hampering the adequate characterization of lesions. Identifying and targeting focal anaplasia or other prognostically relevant tumor areas could significantly enhance the diagnostic and prognostic yield of invasive surgical biopsy.[20] Recently, the issue of performing biopsies in DIPG has become of special interest and has been much debated.[10] Indeed, the advanced MR imaging techniques used here may provide valuable longitudinal information on the evolving tumor biology when used at several time points and thus may enhance our ability to monitor therapeutic responsiveness in this particular pathology in which current therapies—with the exception of radiation—are mainly experimental.

The significance of the phenotypic variations of $T2_{HOF}$ in DIPG is yet unclear. These variations may represent subsequent stages of the process of anaplastic tumor transformation. A previous study suggested that T2 hypointensity itself is associated with worse outcome in DIPG.[10] Another study found that tumors with rCBV values higher than those of GM were associated with a shorter time to progression.[18] In our study, rCBV values of $T2_{HOF}$ and $T2^{HRT}$ were never higher than those of GM. Therefore, a $T2_{HOF}$ associated with an elevated rCBV (ie, higher than $T2^{HRT}$) may be an important factor for prognosis. However, whether patients with $T2_{HOF}$ in our study have a worse outcome than other patients with DIPG is unknown, and we have refrained from a statistical evaluation of the current data because of the small patient sample. Yet, we believe that the concept of the diagnostic imaging evaluation of $T2_{HOF}$ presented in this work may also be applicable to other similar tumors (eg, thalamic gliomas with the exception of juvenile pilocytic astrocytomas) in which stereotactic biopsies before treatment are currently recognized as the standard of care by most clinicians. Studies performed for those tumors may help to further elucidate the histopathologic evolution of $T2_{HOF}$.

Limitations

Our study is retrospective in the strict sense of the term. However, we believe that it meets the criteria of a prospective study in many ways. In our institution, virtually every MR imaging examination is performed within the framework of institutional review board–approved prospectively designed clinical trials/imaging protocols. Accordingly, for our hypothesis-driven research, we used data collected in a standardized fashion. In particular, perfusion (and DWI/DTI) studies were performed in all of our patients with the intent of using those data for research along the lines of the originally stated research objectives of the 2 protocols from which patients were recruited. This allowed us to take advantage of the benefits of a "traditional" prospective investigation scheme, even though the specific research question we tried to address in our study was formulated later. Because patients were recruited from 2 protocols, MR imaging parameters varied slightly over the study period as improvements have been made to imaging techniques, particularly to DSC. Sequence parameters, including field strength, differed among the MR imaging platforms; these differences may have had an impact on our results, too. However, our study was primarily designed to compare tumor components within the same patient, which minimized the likelihood of possible errors arising from the use of different imaging parameters.

Conclusions

The findings in this study support our hypothesis that $T2_{HOF}$ may indeed correspond to areas of focal anaplasia, because increased rCBV likely reflects a global expansion of the intralesional blood pool secondary to tumor-induced angioneogenesis, and low ADC likely corresponds to increased tumor cellularity. $T2_{HOF}$ is more common in DIPG than originally suspected. $T2_{HOF}$ may be the ideal target when stereotactic biopsy of tumors that present with an inhomogeneous T2 signal intensity is considered.

Acknowledgments

We thank Cherise Guess, MD, Department of Scientific Editing, St. Jude Children's Research Hospital, for the many helpful suggestions to improve this manuscript.

References

1. CBTRUS. Central Brain Tumor Registry of the United States. CBTRUS statistical report: primary brain and central nervous system tumors diagnosed in the United States in 2004–2006, February 2010. http://www.cbtrus.org/2010-NPCR-SEER/CBTRUS-WEBREPORT-Final-3–2-10.pdf. Accessed XXX.
2. Albright AL, Price RA, Guthkelch AN. **Brain stem gliomas of children: a clinicopathological study.** *Cancer* 1983;52:2313–19
3. Epstein F, Wisoff JH. **Intrinsic brainstem tumors in childhood: surgical indications.** *J Neurooncol* 1988;6:309–17
4. Kaplan AM, Albright AL, Zimmerman RA, et al. **Brainstem gliomas in children: a Children's Cancer Group review of 119 cases.** *Pediatr Neurosurg* 1996;24:185–92
5. Mantravadi R, Phatak R, Bellur S, et al. **Brain stem gliomas: an autopsy study of 25 cases.** *Cancer* 1982;49:1294–96
6. Yoshimura J, Onda K, Tanaka R. **Clinicopathological study of diffuse type brainstem gliomas: analysis of 40 autopsy cases.** *Neurol Med Chir (Tokyo)* 2003;43:375–82, discussion 382
7. Packer R, Allen J, Nielsen S. **Brainstem glioma: clinical manifestations of meningeal gliomatosis.** *Ann Neurol* 1983;14:177–82
8. Silbergeld D, Berger M, Griffin B, et al. **Brainstem glioma with multiple intraspinal metastases during life: case report and review of the literature.** *Pediatr Neurosci* 1988;14:103–07
9. Lach B, Al Shail E, Patay Z. **Spontaneous anaplasia in pilocytic astrocytoma of cerebellum.** *Br J Neurosurg* 2003;17:250–52
10. Leach PA, Estlin EJ, Coope DJ, et al. **Diffuse brainstem gliomas in children: should we or shouldn't we biopsy?** *Br J Neurosurg* 2008;22:619–24
11. Hakyemez B, Erdogan C, Ercan I, et al. **High-grade and low-grade gliomas: differentiation by using perfusion MR imaging.** *Clin Radiol* 2005;60:493–502
12. Humphries PD, Sebire NJ, Siegel MJ, et al. **Tumors in pediatric patients at diffusion-weighted MR imaging: apparent diffusion coefficient and tumor cellularity.** *Radiology* 2007;245:848–54
13. Law M, Yang S, Babb JS, et al. **Comparison of cerebral blood volume and vascular permeability from dynamic susceptibility contrast-enhanced perfusion MR imaging with glioma grade.** *AJNR Am J Neuroradiol* 2004;25:746–55
14. Law M, Yang S, Wang H, et al. **Glioma grading: sensitivity, specificity, and predictive values of perfusion MR imaging and proton MR spectroscopic imaging compared with conventional MR imaging.** *AJNR Am J Neuroradiol* 2003;24:1989–98
15. Rumboldt Z, Camacho DLA, Lake D, et al. **Apparent diffusion coefficients for differentiation of cerebellar tumors in children.** *AJNR Am J Neuroradiol* 2006;27:1362–69
16. Stadlbauer A, Gruber S, Nimsky C, et al. **Preoperative grading of gliomas by using metabolite quantification with high-spatial-resolution proton MR spectroscopic imaging.** *Radiology* 2006;238:958–69
17. Jain JJ, Glass JO, Reddick WE. **Automated arterial input function identification using self organized maps.** In: *Proceedings of the SPIE International Symposium on Medical Imaging: Image Processing Conference,* San Diego, California. February 15–20, 2007
18. Fuss M, Wenz F, Essig M, et al. **Tumor angiogenesis of low-grade astrocytomas measured by dynamic susceptibility contrast-enhanced MRI (DSC-MRI) is predictive of local tumor control after radiation therapy.** *Int J Radiat Oncol Biol Phys* 2001;51:478–82

19. Ostergaard L, Weisskoff RM, Chesler DA. **High resolution measurement of cerebral blood flow using intravascular tracer bolus passages. Part I. Mathematical approach and statistical analysis.** *Magn Reson Med* 1996;36:715–25
20. Chaskis C, Stadnik T, Michotte A, et al. **Prognostic value of perfusion-weighted imaging in brain glioma: a prospective study.** *Acta Neurochir (Wien)* 2006;148:277–85, discussion 285. Epub 2006 Jan 19
21. Ellison D. **Classifying the medulloblastoma: insights from morphology and molecular genetics.** *Neuropathol Appl Neurobiol* 2002;28:257–82
22. Sugahara T, Korogi Y, Kochi M. **Usefulness of diffusion-weighted MRI with echoplanar technique in the evaluation of cellularity in gliomas.** *J Magn Reson Imaging* 1999;9:53–60
23. Inoue T, Ogasawara K, Beppu T. **Diffusion tensor imaging for preoperative evaluation of tumor grade in gliomas.** *Clin Neurol Neurosurg* 2005;107:174–80
24. Helton KJ, Phillips NS, Khan RB, et al. **Diffusion tensor imaging of tract involvement in children with pontine tumors.** *AJNR Am J Neuroradiol* 2006;27:786–93
25. Helton KJ, Weeks JK, Phillips NS, et al. **Diffusion tensor imaging of brainstem tumors: axonal degeneration of motor and sensory tracts.** *J Neurosurg Pediatr* 2008;1:270–76
26. Lee CE, Danielian LE, Thomasson D, et al. **Normal regional fractional anisotropy and apparent diffusion coefficient of the brain measured on a 3 T MR scanner.** *Neuroradiology* 2009;51:3–9
27. Löbel U, Sedlacik J, Güllmar D, et al. **Diffusion tensor imaging: the normal evolution of ADC, RA, FA, and eigenvalues studied in multiple anatomical regions of the brain.** *Neuroradiology* 2009;51:253–63
28. Law M, Young RJ, Babb JS, et al. **Gliomas: predicting time to progression or survival with cerebral blood volume measurements at dynamic susceptibility-weighted contrast-enhanced perfusion MR imaging.** *Radiology* 2008;247:490–98
29. Al-Okaili RN, Krejza J, Woo JH, et al. **Intraaxial brain masses: MR imaging-based diagnostic strategy—initial experience.** *Radiology* 2007;243:539–50
30. Arvinda HR, Kesavadas C, Sarma PS, et al. **Glioma grading: sensitivity, specificity, positive and negative predictive values of diffusion and perfusion imaging.** *J Neurooncol* 2009;94:87–96
31. Shin JH, Lee HK, Kwun BD, et al. **Using relative cerebral blood flow and volume to evaluate the histopathologic grade of cerebral gliomas: preliminary results.** *AJR Am J Roentgenol* 2002;179:783–89
32. Tong KA, Ashwal S, Obenaus A, et al. **Susceptibility-weighted MR imaging: a review of clinical applications in children.** *AJNR Am J Neuroradiol* 2008;29:9–17